BeppoSAX broad-band observations of low-redshift quasars: spectral curvature and iron K$_\alpha$ lines

T. Mineo[1], **F. Fiore**[2,3,4], **A. Laor**[5], **E. Costantini**[4,6], **W.N. Brandt**[7], **A. Comastri**[6], **R. Della Ceca**[8], **M. Elvis**[4], **T. Maccacaro**[8], **and S. Molendi**[9]

[1] Istituto di Fisica Cosmica ed Applicazioni all'Informatica CNR, Via U. La Malfa 153, 90146 Palermo, Italy
[2] BeppoSAX Science Data Center, c/o Telespazio, Via Corcolle 19, 00131 Roma, Italy
[3] Osservatorio Astronomico di Roma, 00040 Monteporzio (Rm), Italy
[4] Harvard Smithsonian Center for Astrophysics, Cambridge, MA, USA
[5] Physics Department, Technion, Haifa 32000, Israel
[6] Osservatorio Astronomico di Bologna, Via Ranzani 1, 40127 Bologna, Italy
[7] Department of Astronomy and Astrophysics, The Pennsylvania State University, 525 Davey Lab, University Park, PA 16802, USA
[8] Osservatorio Astronomico di Brera, Via Brera 28, 20121 Milano, Italy
[9] Istituto di Fisica Cosmica e Tecnologia Relative CNR, Via Bassini 15, 20133 Milano, Italy

Abstract. We present results from BeppoSAX observations of 10 low redshift quasars. The quasars are part of the Laor et al. (1997) sample of 23 optically selected PG quasars with redshift < 0.4 and low Galactic absorption along the line of sight. Significant spectral curvature is detected for the 6 quasars with the highest signal to noise ratio in their low energy spectra. The average curvature can be parameterized as a flattening of the underlying power law by $\Delta\alpha \sim 0.5$ above ~ 1 keV. We find that quasars with a steeper soft X-ray (0.1–2 keV) spectrum tend to be steeper also at higher (2–10 keV) energies. The distribution of the best fit 2–10 keV slopes is similar to that found for other radio-quiet AGN and characterized by a large dispersion around the mean: $\alpha_E \simeq 1.0 \pm 0.3$. Iron K$_\alpha$ lines are detected in 4 quasars. In the narrow–line quasar PG 1115+407, the rest frame line energy (6.69±0.11 keV) and equivalent width (580±280 eV) are consistent with those found in a few low redshift narrow–line Seyfert 1 galaxies (NLSy1). This, together with the similarity of the 0.1–10 keV X-ray continuum, suggests that this quasar is the higher redshift and luminosity analog of a NLSy1. In the broad line quasar PG 0947+396, the rest-frame line energy suggests fluorescence from cold iron. The line equivalent width (> 400 eV) is however about 2–3 times higher than that usually found in Seyfert 1 galaxies. The high energy power-law slopes and the iron line emission properties seem to be unrelated to the X–ray luminosity.

Key words: galaxies: quasars: general – galaxies: quasars: emission lines – X-rays: galaxies

1. Introduction

Observations of quasars above 2 keV have in the past been largely devoted to objects selected via X-rays. Their 2–10 keV spectral indices cluster tightly around a "canonical" value of 0.9 ($f_E \propto E^{-\alpha}$; Williams et al. 1992, Comastri et al. 1992, Reeves et al. 1997, Lawson & Turner 1997). This uniformity may be the result of a selection effect (Elvis 1992). Seyfert galaxies, in fact, do indeed show a significantly wider range of 2–10 keV spectral indices (Brandt et al. 1997) and QSOs might show the same effect as reported by recent studies of ASCA observations (George et al. 2000). We have therefore started a program to observe, with BeppoSAX (Boella et al. 1997a), a reasonably large, well defined, and representative sample of optically selected quasars. Our goals are to perform a systematic study of their hard ($E > 2$ keV) emission spectra and, taking advantage of the broad BeppoSAX band, to compare them with the soft 0.1–2 keV spectra acquired simultaneously.

BeppoSAX has so far observed 10 quasars extracted from the Laor et al. (1997) sample, nine as part of a Core Program and one as part of the Science Verification Phase (SVP). The Laor et al. sample consists of 23 PG quasars selected to have $z < 0.4$, Galactic $N_H < 1.9 \times 10^{20}$ cm^{-2} and $M_B < -23$. These quasars all have good ROSAT PSPC X-ray spectra, radio fluxes, IR photometry, high S/N optical spectro photometry, IUE and HST spectra (Laor et al. 1997 and references therein).

The 0.2–2 keV PSPC spectra of most of these 23 quasars are well fitted by a single power law plus Galactic absorption. The average spectral index is $\alpha_E = 1.62 \pm 0.45$, and the α_E range is 0.9–2.8. The large spread in α_E permitted the discovery of correlations between the soft X-ray spectral shape and optical emission line properties (Laor et al. 1994, 1997, Boller et al. 1996, Ulrich-Demoulin & Molendi 1996): steeper soft X-ray quasars tend to have narrower H_β lines, fainter [OIII] emission and stronger FeII emission with respect to H_β. Laor et al. (1997) interpret the $\alpha_E - H_\beta$ FWHM anticorrelation in terms of a dependence of α_E on L/L_{Edd}. The line width is inversely proportional to $\sqrt{L/L_{Edd}}$ if the broad line region is virialized and if its size is determined by the central source luminosity (see

Table 1. PG quasars observed by BeppoSAX

Quasar	Other Name	z	N_{H} $(10^{20}\,\mathrm{cm}^{-2})$
PG 0947+396	K 347-45	0.206	1.92
PG 1048+342		0.167	1.74
PG 1115+407		0.154	1.74
PG 1202+281	GQ Comae	0.165	1.72
PG 1226+023	3C 273	0.158	1.68
PG 1352+183	PB 4142	0.158	1.84
PG 1402+261	TON 182	0.164	1.42
PG 1415+451		0.114	0.96
PG 1512+370	4C 37.43	0.371	1.40
PG 1626+554		0.133	1.82

Laor et al. 1997, Sect. 4.7). So narrow-line, steep (0.1–2 keV) spectrum AGNs emit close to the Eddington luminosity (Nicastro 2000).

A proposed scenario for these sources, as described by Pounds et al. (1995), is that the hard X-ray power law is produced by Comptonization in a hot corona: as the object becomes more luminous in the optical-UV, Compton cooling of the corona increases. The corona becomes colder, thus producing a steeper X-ray power law. If this mechanism is operating, then steep α_E(PSPC) quasars should also have a steep hard X-ray power law that would have been missed by hard X-ray surveys. BeppoSAX 0.1–10 keV observations should help in verifying this picture; test if the correlations between the soft X-ray spectrum and the optical lines properties hold also at high X-ray energies; and study the Iron K emission lines in high luminosity objects, to test the claim of an X-ray Baldwin effect (Iwasawa & Taniguchi 1993, Nandra et al. 1997).

In this paper we report the analysis of BeppoSAX observations of 10 PG quasars. In Sect. 2 we describe the observations and the data analysis; in Sect. 3 we present the broad band 0.1–100 keV spectra; in Sect. 4 we discuss in detail the 0.1–10 keV spectral shape and compare it with the PSPC results; in Sect. 5 we present results on the iron line; in Sect. 6 we present our conclusions. A correlation between the 0.1–10 keV spectral shape and the optical line properties is deferred to a future publication.

In the paper H_0=50 km s^{-1} Mpc^{-1} and q_0=0.5 are assumed.

2. Observations and data reduction

Table 1 lists the PG quasars observed by BeppoSAX, together with their redshifts (Schmidt & Green 1983) and 21 cm Galactic column densities (we use the values quoted in Laor et al. 1997, where the relevant references are also reported). PG 1226+023 (3C 273) was observed during the SVP, and a detailed wide band spectral analysis has been published by Grandi et al. (1997).

All quasars but two are radio quiet according to the definition given by Kellermann et al. (1989) based on the ratio R between the radio flux at 6 cm and the optical flux at 4400 Å: radio-loud quasars present $R > 10$. This criterion corresponds to selecting $\alpha_{ro} \leq 0.2$ where α_{ro} is the radio–to–optical spectral index defined as $log(S(5GHz)/S(2500\,\text{Å}))/5.38$ (Stocke et al.

1985). The radio-loud quasars in our sample are PG 1512+370 ($R = 190$; Kellermann et al. 1989) and PG 1226+023 ($R = 1138$; Kellermann et al. 1989).

Table 2 shows the dates, the observing codes and the exposure times for the BeppoSAX observations of the ten PG quasars. These observations were performed with the Narrow Field Instruments, LECS (0.1–10 keV; Parmar et al. 1997), MECS (1.3–10 keV, Boella et al. 1997b), HPGSPC (4–60 keV, Manzo et al. 1997) and PDS (13–200 keV, Frontera et al. 1997). We report here the analysis of the LECS, MECS and PDS data; the HPGSPC has a large and structured background which makes it not sensitive enough for faint extragalactic sources.

At launch the MECS was composed of three identical units. Unfortunately on 1997 May 6th a technical failure caused the unit MECS1 to switch off. All observations after this date were performed with two units (MECS2 and MECS3). The MECS energy resolution is about 8% at 6 keV. The LECS is operated during spacecraft dark time only; therefore LECS exposure times are usually smaller than MECS ones by a factor 1.5–3. The PDS is a collimated instrument with a FWHM of about 1.4 degrees. Since it has a larger field of view than the LECS and MECS ($\sim$ 30 arcmin radius) and no angular resolution, any PDS detection has to be validated by a simultaneous fit with LECS and MECS spectra. The PDS collimators are rocked on and off source every 96 seconds, to simultaneously monitor the background, the PDS on-source time is then typically half of the total integration time.

Standard data reduction was performed using the software package "SAXDAS".[1] In particular, data are linearized and cleaned from Earth occultation periods and unwanted periods of high particle background (satellite passages through the South Atlantic Anomaly). The LECS, MECS and PDS background is relatively small and stable (variations of at most 30% around the orbit) due to the low inclination orbit (3.95 degrees). Therefore, the data quality does not depend strongly on screening criteria such as Earth elevation angle, bright Earth angle or magnetic cut-off rigidity (we accumulated data for Earth elevation angles > 5 degrees and magnetic cut-off rigidity > 6). For the PDS data we adopted an energy and temperature dependent rise-time selection, which decreases the PDS background by $\sim 40\%$. This improves the signal to noise ratio of faint sources by about a factor of 1.5 (Fiore et al. 1999b).

Data from the four PDS units and the three (or two) MECS units have been merged after equalization to produce single MECS and PDS spectra.

We extracted spectra from the LECS and MECS using 6 arcmin and 3 arcmin radius regions respectively for all the quasars but PG 1115+407, PG 1226+023 and PG 1626+554. These radii maximize the signal-to-noise ratio below 1 keV in the LECS and above 2 keV in the MECS. For PG 1115+407 we adopted slightly smaller extraction radii (5.3 arcmin for the LECS and 2.7 arcmin for the MECS) to reduce the contamination of several faint sources near the quasar (Fiore et al. 1998, 1999a). The cumulative intensity of these sources is not negligi-

---

[1] see http://www.sdc.asi.it/software

Table 2. Journal of the BeppoSAX observations

Quasar	Starting Dates (yy mm dd, hh:mm:ss)	Observing Code	Exposure (s)			Rate (10^{-2} counts s^{-1})		
			LECS	MECS	PDS	LECS[a]	MECS[a]	PDS[b]
PG 0947+396	1997 Apr 19, 09:39:44	50124001	10 617	18 507	8 004	3.79±0.20	4.21±0.16	15.7±5.9
PG 1048+342	1997 May 3, 09:46:38	50124002	16 030	32 633	13 323	2.67±0.15	3.38±0.11	<9.0
PG 1115+407	1997 May 2, 09:45:15	50124003	17 337	33 797	14 099	2.62±0.15[c]	1.75±0.08[c]	11.5±4.4
PG 1202+281	1997 Dec 11, 05:38:02	50124006	6 344	18 201	8 085	4.45±0.28	4.27±0.16	<11.6
PG 1226+023	1996 Jul 18, 02:03:25	50021001	11 637	129 886	60 639	61.8±0.7[d]	131.7±0.3[d]	158.9±3.6
PG 1352+183	1998 Jan 31, 15:00:35	50124007	8 713	19 378	9 508	2.61±0.19	1.95±0.11	<13.9
PG 1402+261	1999 Jan 17, 00:18:11	50551002	13 225	33 033	14 983	3.02±0.19.	2.64±0.09	<10.5
PG 1415+451	1998 Jan 22, 01:28:37	50124004	8 571	24 133	10 916	2.13±0.18	1.24±0.08	<13.0
PG 1512+370	1998 Jan 25, 19:17:01	50124008	5 101	18 611	8 805	2.90±0.27	2.25±0.12	<14.3
PG 1626+554	1998 Feb 25, 17:33:13	50551001	9 857	30 366	14 460	6.99±0.28[e]	5.06±0.13	<11.1

[a] whenever not explicitly declared the accumulation radius is 6 arcmin for the LECS and 3 arcmin for the MECS
[b] PDS upper limits are given at the 2 σ level
[c] the accumulation radius is 5.3 arcmin for the LECS and 2.7 arcmin for the MECS
[d] the accumulation radius is 10.7 arcmin for the LECS and 5.3 arcmin for the MECS
[e] the accumulation radius is 5.3 arcmin

ble in comparison to the flux of the quasar. For PG 1626+554 we used a 5.3 arcmin radius region to extract the LECS spectrum in order to avoid contamination from a source at $\sim$ 10 arcmin off-axis. The signal-to-noise ratio for PG 1226+023, the strongest source in our sample, is maximum at 10.7 and 5.3 arcmin respectively for the LECS and the MECS: these radii have been then used to accumulate the spectra.

LECS and MECS internal backgrounds depend on the position within the field of view (see Chiappetti et al. 1998, BeppoSAX Cookbook,[2] Parmar et al. 1998, Fiore et al. 1999b). Accordingly, background spectra were extracted from high Galactic latitude 'blank' fields from the same region of the detectors. We have compared the mean level of the background in these observations with that in the quasar observations using source free regions at various positions in the detectors:

I) In the LECS the mean local background above 1 keV is consistent with the 'blank' field mean background in all cases but PG 1048+342 and PG 1626+554, where the local background is higher by 14 and 7% respectively. The local low energy (0.1–1 keV) background is higher than the 'blank' field 0.1–1 keV background by 30–40% in four cases (PG 1048+342, PG 1415+451, PG 1202+281 and PG 1626+554). The total excess soft background, scaled to the source extraction region, is of the order of 10^{-3} counts s^{-1}.
In all cases but PG 1048+342 and PG 1626+554, we have not modified the 'blank' field background spectra, but we have compared the significance of any feature below 1 keV with the size of the background excess. In PG 1048+342 and PG 1626+554 the 'blank' field background spectra were scaled by the above amount.

II) In the MECS the local background is higher than the 'blank' field background in seven out of ten cases (by 9 to 20%). In all cases the excess was constant with energy. We have

then scaled by the same amount the 'blank' field background spectra before subtraction.

Table 2 gives the detected source count rates in the energy ranges used for the spectral analysis for each instrument; PDS upper limits are given at the 2 σ level. All quasars are detected in the LECS and MECS instruments. A positive detection (better than 2 σ level) is present in the PDS for PG 0947+396, PG 1115+407 and PG 1226+023.

No flux variability has been detected in any of the observed sources, except for PG 1402+261, for which a 10% variation in the MECS total count rate is seen in time scale of the order of 15 ks. The variability reaches 30% in the higher energy range (E>4 keV).

Errors quoted in this paper represent 1 σ uncertainty for 1 interesting parameter ($\Delta\chi^2$=1.0).
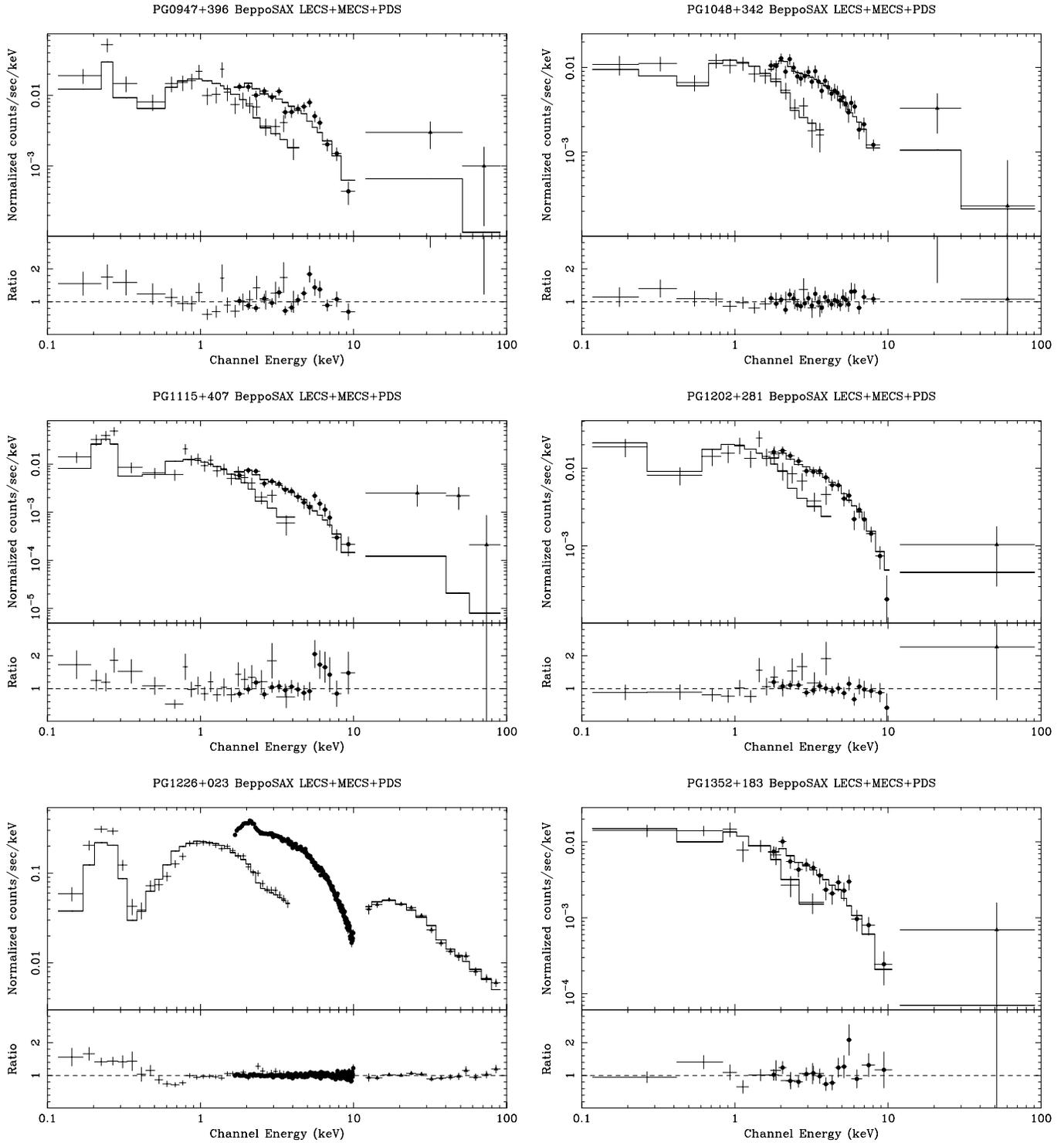
3. 0.1–100 keV spectral analysis

Spectral fits were performed using the XSPEC 9.0 software package and public response matrices issued in November 1998. PG 1226+023 was observed at an off-axis angle of 2 arcmin, in a position close to one of the wires supporting the LECS window. The shadowing of this wire affects the resulting low energy spectrum and an appropriate effective area file for this position was created using the LECS matrix generation "LEMAT" code.[3]

PI channels are rebinned sampling the instrument resolution with the same number of channels at all energies when possible, but with the requirement of having at least 20 counts in each bin. This guarantees the applicability of the χ^2 method in determining the best-fit parameters.

Constant factors have been introduced in the fitting models in order to take into account the intercalibration systematic uncertainties between instruments (BeppoSAX Cookbook, Fiore et al. 1999b). In the fits we use the MECS as reference instru-

---

[2] see http://www.sdc.asi.it/software/cookbook

[3] see http://www.sdc.asi.it/software/saxdas/lemat.html

Fig. 1. Joint LECS (crosses), MECS (filled circles) and PDS (triangles) spectra of the ten PG quasars fitted with a single power law plus Galactic absorption (continuous curve). In each panel, the lower portion reports the data-to-model ratios.

ments and constrain the LECS and PDS parameters to vary in the range 0.7–1 and 0.77–0.95 respectively.

The energy ranges used for the fits are: 0.1–4 keV for the LECS (channels 11–400), 1.65–10 keV for the MECS (channels 37–220) and 15–100 keV for the PDS.

LECS, MECS and PDS spectra of the PG quasars were first fitted with a single power law of the form $f_E = e^{-N_H \sigma(E)} f_o E^{-\alpha}$, where f_E is the flux density, $\sigma(E)$ is the absorption cross section per H atom (Morrison & McCammon 1983), f_o is the flux density at 1 keV, α is the energy index and
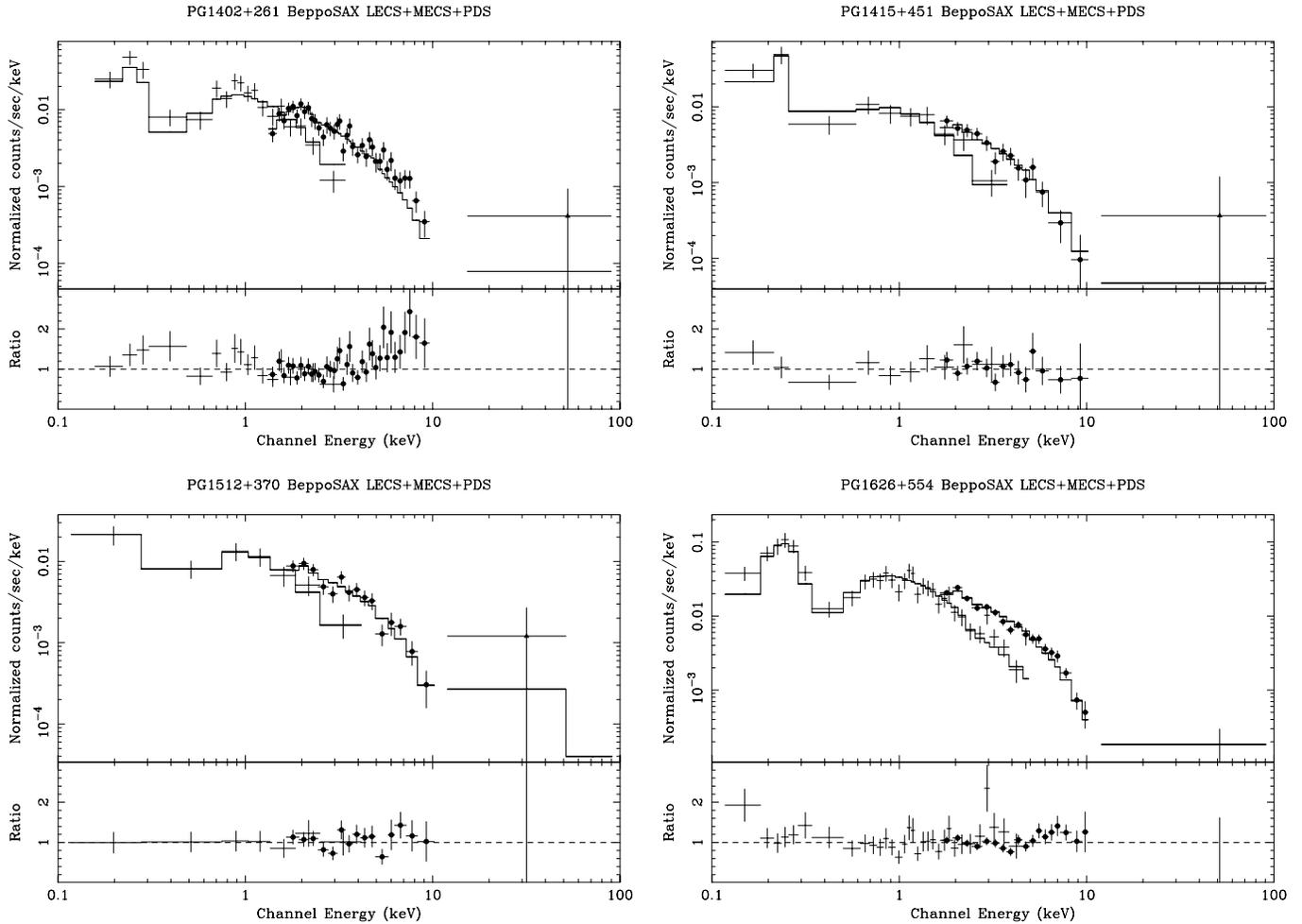
Fig. 1. (continued)

E is in units of keV. The absorbing column $N_{\rm H}$ has been fixed to its Galactic value. Fig. 1 shows the spectra along with the best fit power-law model and the residuals expressed as data-to-model ratio. Inspection of this figure allows one to note that features are present in the 1–10 keV residuals of most of the spectra, as it will be discussed in detail in the next section. For all quasars but PG 0947+396 and PG 1115+407, the PDS points are fully consistent with LECS–MECS extrapolations.

The PDS detections in PG 0947+396 and PG 1115+407 are well above the LECS–MECS relative extrapolations. This excess could be due to serendipitous sources present in the large (1°4 FWHM) PDS field of view: confusion ultimately limits our capability to constrain the high-energy spectrum. The chance of finding a source in the PDS beam area can be evaluated using the HEAO–1 A4 results and assuming a $logN - logS$ slope of -1.5. The HEAO–1 A4 all sky catalog (Levine et al. 1984) lists just 7 high Galactic latitude sources in the 13–80 keV band down to a flux of 2×10^{-10} erg cm^{-2} s^{-1} (10mCrab). Extrapolating this number of sources to the average flux 1.3×10^{-11} erg cm^{-2} s^{-1} detected in the energy band 15–100 keV, a chance coincidence rate of $\simeq 2\%$ per target position is expected in the PDS at high Galactic latitude (Elvis et al. 2000). We also

searched the NED and Simbad catalogs for possible sources that might contribute to the PDS detection. The Seyfert 1 galaxy MS 1112.5+4059 lies at about 40 arcmin from PG 1115+407. Its X-ray 0.3–3.5 keV flux was about 1.5×10^{-12} erg cm^{-2} s^{-1} during the Einstein observation (Stocke et al. 1991). Moreover, a PSPC observation of this source shows a steep spectrum (α=1.61), with flux variability of less than 40% (Ciliegi & Maccacaro 1996, 1997). Unless a large variation (factor of 10) or a sharp hardening of the spectrum above 3 keV (not usually observed in Seyfert 1 galaxies) occurred, this object cannot be the responsible for the PDS flux detected. At about 80 arcmin from the quasar there is also the Abell cluster A1190, which has a diameter of about 40 arcmin putting part of its emission within the PDS field of view (FOV). Its 2–10 keV flux is 3.6×10^{-12} erg cm^{-2} s^{-1} (Ebeling et al. 1996). Again, unless a very hard component dominates the spectrum above 10 keV, this object cannot be responsible for the PDS flux. Three quasars have been recently discovered by Fiore et al. (1999a) within 6 arcmin of PG 1115+407 at redshifts 0.4–1.3. Their 2–10 keV flux is however at least 10 times smaller than that of the PG quasar and therefore they are unlikely to contribute to the PDS flux, unless their spectrum is strongly inverted.

Table 3. Results of the fit of LECS and MECS spectra with a single power law

Quasar	Fit[a]	$N_{\rm H}^{\rm b}$	Energy Index	$F_{0.1-2}^{\rm c}$	$F_{2-10}^{\rm c}$	$L_{2-10}^{\rm d}$	$\chi^2_{\rm pw}$(dof)	F_{15-100}^{f}
PG 0947+396	1	0.57±0.35	0.85±0.07	2.68±0.16	2.49±0.10	4.9	53.4 (32)	1.58±0.59
	2	1.92	0.97±0.07				71.7 (33)	
PG 1048+342	1	1.08±0.42	0.82±0.07	1.96±0.13	2.09±0.07	2.7	23.4 (38)	<0.94
	2	1.74	0.87±0.06				25.6 (39)	
PG 1115+407	1	0.34±0.32	1.29±0.09	2.72±0.16	0.93±0.04	1.0	40.8 (33)	0.96±0.36
	2	1.74	1.51±0.07				54.2 (34)	
PG 1202+281	1	2.40±0.69	0.97±0.08	2.77±0.22	2.62±0.10	3.3	27.2 (28)	<1.18
	2	1.72	0.92±0.06				28.4 (29)	
PG 1226+023[e]	1	0.88±0.10	0.59±0.06	40.55±0.68	69.80±0.19	80.0	301.3 (207)	16.03±0.04
	2	1.68	0.60±0.05				338.9 (208)	
PG 1352+183	1	1.96±0.61	1.27±0.12	1.98±0.15	1.05±0.07	1.2	22.4 (20)	<1.27
	2	1.84	1.26±0.06				22.6 (21)	
PG 1402+261	1	<0.62	1.24±0.08	1.16±0.24	1.53±0.10	1.9	66.9 (53)	<0.89
	2	1.42	1.40±0.07				70.4 (54)	
PG 1415+451	1	0.52±0.49	1.34±0.14	2.09±0.25	0.69±0.05	0.4	16.2 (21)	<1.12
	2	0.96	1.42±0.09				16.8 (22)	
PG 1512+370	1	1.42±0.69	1.12±0.12	1.97±0.22	1.23±0.07	8.5	16.7 (20)	<1.37
	2	1.40	1.12±0.10				16.7 (21)	
PG 1626+554	1	1.03±0.29	1.17±0.06	5.30±0.26	2.92±0.09	2.4	47.3 (42)	<1.01
	2	1.82	1.25±0.05				52.8 (43)	

[a] Fit 1: $N_{\rm H}$ as free parameter; Fit 2: $N_{\rm H}$ fixed to the Galactic value
[b] 10^{20} cm^{-2};   [c] 10^{-12} erg cm^{-2} s^{-1};   [d] 10^{44} erg s^{-1}
[e] Introducing an edge in the fitting model (2) we get χ^2 = 281.9 (206 dof);
[f] 10^{-11} erg cm^{-2} s^{-1}; PDS fluxes or 2σ upper limits obtained extrapolating the LECS+MECS spectral shapes.

In the case of PG 0947+396 the quasar KUV 09468+3916 lies about 25 arcmin away. The 0.1–2.4 keV flux of this source is about 30% of PG 0947+396 (Yuan et al. 1998) and again it can not easily be responsible of the PDS flux detected.

We conclude that the PDS flux in both observations is most likely dominated by the PG quasars and investigate in Sect. 5 if the presence of a Compton reflection component could justify the excess.

4. 0.1–10 keV spectral analysis

We present in this section the result of the analysis of the LECS and MECS spectra of the sample quasars, and defer to Sect. 5 the inclusion of the PDS data for PG 1115+407 and PG 0947+396.

Two sets of fits have been performed: (1) leaving $N_{\rm H}$ free to vary; and (2) fixing $N_{\rm H}$ to its Galactic value. The best-fit parameters and the χ^2 for each quasar are reported in Table 3 together with the fitted fluxes in the 0.1–2 and 2–10 keV energy bands, with the 2–10 keV luminosity, and with the fluxes or 2σ upper limits measured by the PDS in the energy range 15–100 keV computed extrapolating the LECS-MECS spectral shapes. The χ^2 are generally rather small, not surprisingly, given the relatively modest statistics. Nevertheless, analysis of the residuals shows systematic local deviations below 1 keV, above 5 keV and in the Iron K-α line region, which we discuss in turn.

Positive residuals below 1 keV are evident in Fig. 1 for six of the ten sources: PG 0947+396, PG 1048+342, PG 1115+407, PG 1226+023, PG 1402+261 and PG 1626+554. In all these cases, the fits with $N_{\rm H}$ free to vary gives unphysical values,

smaller than the Galactic column along the line of sight. The decrease of the χ^2 between model (1) and model (2) for the six quasars is significant at the 99.8, 93.4, 99.8, >99.9, 90.0, and 96.7% level respectively. Two of these quasars (PG 1048+342 and PG 1626+554) also have a residual background excess (see previous section). However the excess of LECS counts below 1 keV with respect to the best fit power-law model is 2–5 times higher than the residual background excess: 1.5×10^{-3} counts s^{-1} against 3×10^{-4} counts s^{-1} in PG 1626+554, 1.0×10^{-3} counts s^{-1} against 5×10^{-4} counts s^{-1} in PG 1048+342. We are therefore confident that in all six quasars the excess of counts below 1 keV is real.

The case of PG 1626+554 looks rather interesting showing an unusual large excess below 0.2 keV; we further discuss this possibility in the next section.

PG 1402+26 clearly shows the presence of a hard tail (E >5 keV) which is statistically more significant than the soft excess (see Fig. 1) making the χ^2 variation between model (1) and model (2) marginally significant (90%). PG 1626+554 also shows an excess with respect to a simple power law above 5 keV, but, with a lower statistical significance.

We have then fitted the LECS and MECS spectra of the quasars with a broken power-law model:

$$f_E = e^{-N_{\rm H}\sigma(E)} f_o E^{-\alpha_1} \qquad\qquad E \leq E_{br}$$
$$f_E = e^{-N_{\rm H}\sigma(E)} f_o E_{br}^{-(\alpha_1-\alpha_2)} E^{-\alpha_2} \quad E \geq E_{br}$$

The absorbing column $N_{\rm H}$ has been fixed to the Galactic value. In fact, leaving it as a free parameter gives values fully compatible with the Galactic ones but strongly increases the error on the

Table 4. Results of the fit with a broken power law

Quasar	PSPC Energy Index	Energy Index Soft	Energy Index Hard	BeppoSAX E_{br} (keV)	χ^2_{bpw}(dof)	$F(\chi^2_{\mathrm{pw}}, \chi^2_{\mathrm{bpw}})$
PG 0947+396	1.51±0.02	1.42±0.16	0.80±0.08	1.09±0.34	48.8 (31)	0.997
PG 1048+342	1.39±0.05	1.09±0.16	0.79±0.07	1.10±0.69	22.0 (37)	0.935
PG 1115+407	1.89±0.04	2.15±0.43	1.26±0.10	0.64±0.32	36.9 (32)	0.998
PG 1202+281	1.22±0.02	0.70±0.19	0.99±0.06	1.0	26.6 (28)	0.821
PG 1226+023[a]	0.94±0.01	1.03±0.3	0.61±0.01	0.55±0.30	253.1 (204)	>0.999
PG 1352+183	1.52±0.03	1.29±0.15	1.20±0.13	1.0	22.3 (20)	0.390
PG 1402+261	1.93±0.03	1.59±0.10	0.52±0.30	3.4±0.5	43.2 (52)	>0.999
PG 1415+451	1.74±0.04	1.37±0.15	1.49±0.16	1.0	16.5 (21)	0.467
PG 1512+370	1.21±0.04	1.12±0.21	1.12±0.13	1.0	16.7 (20)	–
PG 1626+554	1.94±0.04	1.52±0.21	1.16±0.06	0.78±0.46	47.0 (41)	0.903

[a] The fitting model includes an absorbing edge (see text)

soft energy index. The evaluation of the harder spectral index based essentially on MECS data is not affected by the different source redshifts: the MECS effective area varies only slowly in the range 2.5–7 keV.

The reduction in χ^2 between the broken power-law and the single power-law fit is significant in PG 0947+396 (99.7%), PG 1115+407 (99.8%) and PG 1402+261 (99.9%), again confirming significant curvature in the spectra of these quasars. It is marginally significant in PG 1626+554 (90.3%) and PG 1048+342 (93.5%). In the case of PG 1226+023 we have also introduced in the model an absorbing edge to account for the 0.5–1 keV feature (Grandi et al. 1997). The improvement in χ^2 between the broken power-law+edge model and the power-law+edge model is significant at the 99.998% level. The parameters of the absorbing edge are E=0.64±0.07 keV and $\tau = 0.74 \pm 0.21$, consistent with the results of Grandi et al. (1997) and Orr et al. (1998).

For the other four quasars the fit gives a χ^2 similar to the single power-law fit, and the break energy is ill-defined. To obtain low and high energy indices to be compared with those of the quasars with significant curvature we repeated the fits of the PG 1202+281, PG 1352+183, PG 1415+451, PG 1512+370 spectra fixing the break energy at 1 keV. We also tried other different values of break energy between 0.5 and 1.5 keV and, as expected, no significant variations in the fitting parameters and in the χ^2 can be detected. The parameters relative to the fits and the F-tests for the χ^2 variations from the single power-law fits are reported in Table 4 along with the best fit power-law PSPC energy index. Note that the break energy in the PG 1402+261 fit is significantly higher than found for the others, as expected from the presence of the hard tail.

Fig. 2 shows the soft energy indices (α_S(BSAX)) vs the hard ones (α_H); points marked with squares represent the six quasars where spectral curvature may be present.

We plot in Fig. 3 BeppoSAX soft energy index (α_S(BSAX)) as a function of the PSPC one (α_S(PSPC)). A systematic shift between the BeppoSAX measurements and the PSPC ones is evident; this can be modeled as a constant difference of $\Delta\alpha_E = -0.27 \pm 0.03$ between the two spectral indices. This difference
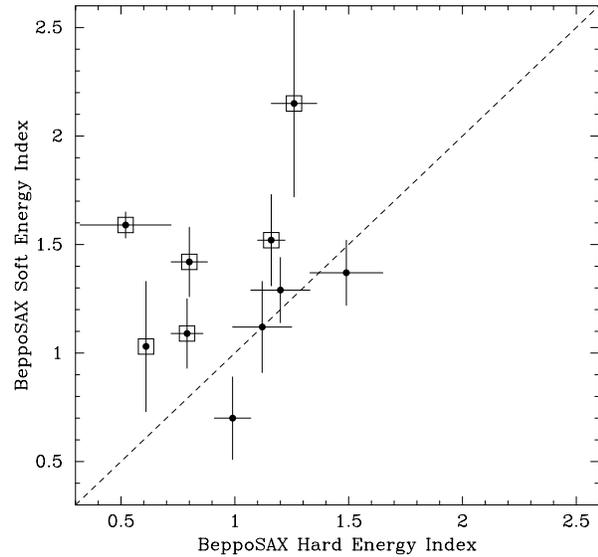
Fig. 2. BeppoSAX soft energy indices α_S(BSAX) vs the hard ones α_H for the observed quasars. Points marked with squares represent the six quasars where a spectral curvature is present and the dashed line identifies the locus of α_S(BSAX)=α_H

could be due to the differences between the LECS and PSPC response functions coupled with low energy spectral steepening of the intrinsic quasar emission, or it may be due to calibration errors in one of the two detectors. A more detailed comparison of the PSPC and LECS results is described in the Appendix. Fig. 4 shows α_S(PSPC) vs α_H.

We also fitted the quasar spectra in which a soft excess is detected with other composite models: a double power law of the form $f_E = e^{-N_H \sigma(E)}(f_S E^{-\alpha_S} + f_H E^{-\alpha_H})$, a power law plus blackbody and a power law plus bremsstrahlung. In all cases the quality of the fits is acceptable and does not allow us to discriminate between models. Moreover the uncertainties in the soft component parameters are quite large. Fits with a power law plus bremsstrahlung always give large upper limits on the temperatures. In Table 5 results from the other two models are reported. In particular, we show the two energy indices and the

Table 5. Results of composite fits on quasars with a detection of soft excess

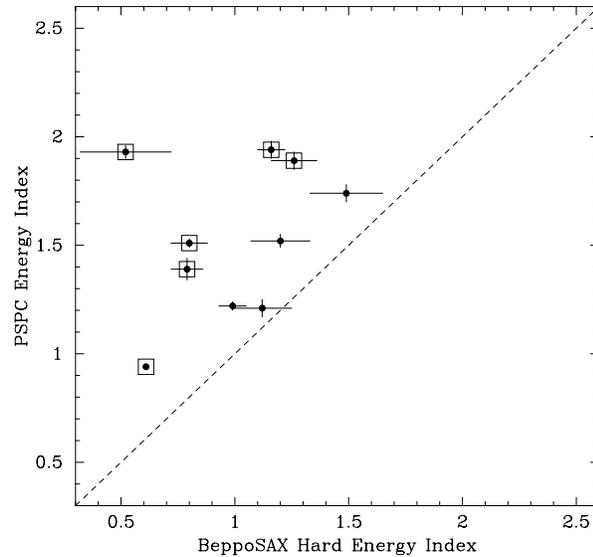| Quasar	Double power law				Power–law plus Blackbody		
	α_S	α_H	E_c (keV)	χ^2 (dof)	kT (keV)	α_H	χ^2 (dof)
PG 0947+396	2.41±1.17	0.77±0.16	0.34	51.0 (31)	0.08±0.02	0.86±0.08	51.1 (31)
PG 1048+342	1.75±1.95	0.73±0.34	0.25	22.4 (37)	0.09±0.02	0.79±0.07	22.1 (37)
PG 1115+407	3.92±1.80	1.25±0.11	0.27	38.8 (32)	0.05±0.02	1.27±0.07	37.3 (32)
PG 1226+023[a]	1.69±0.61	0.58±0.04	0.14	252.0 (204)	0.04±0.02	0.61±0.01	253.4 (204)
PG 1402+261	1.78±0.07	0.52	3.1	51.0 (53)	<0.14	1.35±0.05	58.3 (54)
PG 1626+554	3.73±3.54	1.19±0.06	0.19	43.5 (39)	0.07±0.02	1.19±0.06	43.3 (39)

[a] The fitting models include an absorbing edge
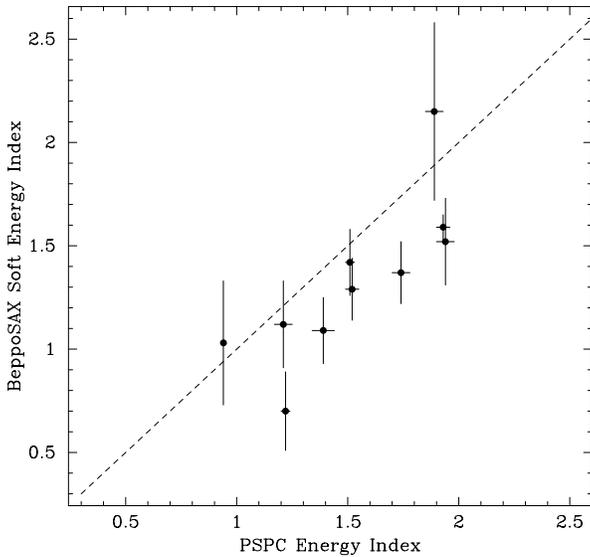
Fig. 3. BeppoSAX soft energy indices α_S(BSAX) vs the PSPC ones α_S(PSPC) for the observed quasars. The dashed line identifies the locus of α_S(BSAX)=α_S(PSPC)

Fig. 4. PSPC energy indices α_S(PSPC) vs BeppoSAX α_H for the observed quasars. Points marked with squares represent the six quasars where a spectral curvature is present and the dashed line identifies the locus of α_S(PSPC)=α_H

energy where the two components have the same flux (E_c) for the double power-law model and the kT and the energy index for power law plus blackbody.

4.1. Spectral curvature

The distribution of the measured spectral indices is the result of the convolution of the parent distribution with the error distribution. Assuming that both distributions can be described by a gaussian, it is possible to deconvolve them to obtain the best estimate of the intrinsic dispersion using a maximum likelihood technique as explained in Maccacaro et al. (1988). The intrinsic dispersions of α_S(BSAX), α_S(PSPC) and α_H are then 0.22±0.14, 0.33±0.12 and 0.25±0.17 respectively, where errors are at the 90% confidence level. We find that intrinsic dispersion is present both in the soft and high energy spectral indices.

We have divided the quasar sample into two groups depending on the α_S(BSAX) value: $\alpha_S < 1.2$ (4 quasars) and $\alpha_S > 1.2$ (6 quasars) and computed the averages applying the same maximum likelihood technique:

α_S(BSAX)=0.98±0.13, α_H=0.85±0.18, α_S(PSPC)=1.19±0.14

for the first group and,

α_S(BSAX)=1.51±0.08, α_H=1.08±0.20, α_S(PSPC)=1.75±0.12

for the second one. Quasars with a steeper soft energy spectrum also tend to be steeper at high energy, although the two mean high energy indices differ only at the 68% confidence level. High energy observations for a larger quasar sample are clearly needed to strengthen this conclusion.

The residuals from fitting a simple power law plus Galactic absorption to the PG 1626+554 spectrum presented in Fig. 1 seem to show what appears to be an unusually large excess at 0.2 keV. We investigated this feature in the PSPC spectrum. This source has the highest soft X-ray to optical flux ratio in Laor et al. sample (mid panel of Fig. 3 of Laor et al. 1997). Moreover, the fit with a free N_H (Table 3 of that paper) gives an absorption column lower than the Galactic one reducing the χ^2 significantly. Fitting independently LECS and PSPC spectra in

Table 6. Results of the MECS data fit with a single power law plus line

Quasar	Fit[a]	z	Energy Index	E_{line} (keV)	EW (eV)	χ^2 (dof)
PG 0947+396	1	0.206	0.85±0.09	–	–	32.5 (14)
	2		0.95±0.10	6.35±0.13	670±170	17.3 (12)
PG 1115+407	1	0.154	1.29±0.12	–	–	14.1 (14)
	2		1.40±0.13	6.69±0.11	580±280	7.8 (12)
PG 1226+023	1	0.158	0.60±0.06	–	–	233.9 (182)
	2		0.60±0.06	6.21±0.09	30±20	219.1 (180)
PG 1352+183	1	0.158	1.16±0.14	–	–	14.1 (13)
	2		1.30±0.16	6.43±0.16	760±460	8.4 (11)

[a] Fit 1: power law plus Galactic absorption; Fit 2: same as Fit 1 plus a narrow line with energy relative to the quasar frame.

the energy range 0.1–1.5 keV gives good χ^2 values (11.5 for 15 dof in the LECS and 24.8 for 26 dof in the PSPC) but incompatible spectral index 1.43±0.10 and 1.94±0.04 respectively. Note however that the BeppoSAX spectral index is compatible with that measured by the PSPC leaving N_H as free parameter (Table 3 of Laor et al.) A highly curved soft X-ray spectrum could explain the large discrepancy between the PSPC and the LECS. An "ultra soft" excess below 0.3 keV could be hinted in this object and we are probably observing the tail of a very steep unusually strong thermal component. Moreover, this "ultra soft" excess could be related to the unusually flat optical-to-soft X-ray slope α_{os}=-1.139 (Laor et al. 1997).

5. High energy features

5.1. Iron K–lines

High energy residuals suggesting the presence of spectral features around 5–6 keV (in the observer's frame) have been observed in several sources: PG 0947+396, PG 1115+407 and PG 1352+183 (see Fig. 1).

An Iron K–line has previously been detected in PG 1226+023 at an energy compatible with the values of many Seyfert 1 galaxies but with a much lower equivalent width (30±20 eV).

To investigate the statistical significance of the high energy features, we fitted the MECS spectra of the three quasars with a power law and then with a power law plus a narrow line. Results are given in Table 6 together with the source redshift. Fig. 5 shows in the upper panels the source spectra fitted with a single power law along with the background and in the lower panel the residuals as data-to-model ratio. Note the excess of counts at about 5.8 keV in PG 1115+407, 5.2 keV in PG 0947+396 and 5.6 keV in PG 1352+183. These excesses do not coincide with the largest features in the background (at about 5.0 and 6.0 keV). Moreover the presence of these excesses cannot be justified by a simple statistical coincidence. In fact the probability to get only one of them with the observed significance by chance is less than 3% and looking at a 10 BL Lac sample observed by BeppoSAX (Wolter et al. 1998) with similar statistical significance we note that no features in the range 5–6 keV are present.

The inclusion of a narrow line at 6.4 keV (quasar frame) is significant at the 97.7% and 96.9% (using the F-test) in PG 0947+396, and PG 1352+183 respectively. This suggests fluorescence from cold iron for the origin of the line, similar to what is found in many local Seyfert 1 galaxies (e.g. Nandra et al. 1997). The equivalent widths are however large (670±170 eV and 760±460 eV), compared to those found in lower redshift Seyfert 1 galaxies (100–200 eV). In PG 1352+183 the uncertainty is large and the EW could be consistent with that of local Seyfert 1 galaxies. In PG 0947+396 the statistics is better, the count rate between 4–6 keV is about ten times that in the background, and the measured EW is $> 200~eV$ also at the 2.7 σ level. We therefore investigated whether the high line equivalent width is the results of fitting a simple power-law model to a complex spectrum. We tried fits with a partial covering model, a broken power law with a break around 5 keV and a power law plus Compton reflection model (see also next section), but in all cases there is no significant reduction in the χ^2. In all cases the line is still required and its equivalent width is never smaller than 400 eV. Note that this object shows only weak UV absorption (Brandt et al. 2000) and no strong X-ray absorption is expected to be present unless it is highly variable: the presence of partial covering absorption would have been difficult to justify.

In PG 1115+407 the inclusion of a line gives an energy 6.7±0.1 keV (probability of 97.0% using the F-test). It is however interesting to note that its energy and equivalent width (580±280 eV) are similar to those found in Narrow line Seyfert 1 galaxies (TON S 180; Comastri et al. 1998, Turner et al. 1998) and consistent with the EW expected from ionized gas. Moreover the low and high energy slopes are similar to those of TONS 180, and the H_β FWHM is only 1720 km s^{-1}, suggesting that PG 1115+407 may be a narrow–line Seyfert 1 galaxy at higher redshift.

Upper limits at 90% confidence level on narrow line equivalent widths at 6.4 and 6.7 keV in all other quasars are also computed: values range between 170 and 770 eV.

5.2. High energy spectra

PG 0947+396 and PG 1115+407 show a signal at $> 2\sigma$ in the PDS that can likely be attributed to the two quasars. We therefore

investigate whether a Compton reflection model from a neutral slab (model **pexrav** in XSPEC) could justify the two detections. In both cases the PDS detection was always above the model despite the best fit normalization for the Compton reflection component was at the limit of the allowed range (R_{cp}=5 is the limit for the reflection component scaling factor). The reduction in χ^2 was never significant.

We also tried to fit the hard excess in PG 1402+26 and PG 1626+554 with the Compton reflection component including the PDS upper limits. The disk inclination has been arbitrarily fixed to 45° and a narrow line at fixed energy has been included into the model. For PG 1402+26 we get a spectral index of 1.62±0.07, a scaling factor for the reflection component (R_{cp}) of 3.8±2.2 and a 2 σ upper limit of 350 eV for the EW of the 6.4 keV iron line. The χ^2 for this model (42.8 for 49 dof) decreases with respect to the value obtained for the simple power law in the 0.1–100 keV range (45.9 for 50 dof) with a significance of 96%.

For PG 1626+554 we get a spectral index of 1.38±0.06, a scaling factor of 2.2±1.1 and a 2 σ upper limit of 400 eV for the EW of the 6.4 keV iron line. The reduction in χ^2 with respect to the simple power law (49.3 for 46 dof with respect to 53.1 for 47 dof) corresponds to a significance level of 93%.

6. Conclusions

We presented the spectral analysis of the BeppoSAX observations of 10 PG quasars selected from the Laor et al. (1997) sample. The main results can be summarized as follows:

- Together with PG 1226+023 a positive detection of the continuum in the 15–100 keV energy range has been found in two more quasars: PG 0947+396 and PG 1115+407. However, a possible contamination from hard serendipitous sources in the PDS field of view cannot be ruled out with the present data.
- The distribution of the 2–10 keV power law energy indices is similar to that observed in other quasars samples. The dispersion around the average value of $\alpha_E = 1.0 \pm 0.3$ reflects the large spread of the best–fit values over the range $0.5 < \alpha_E < 1.5$.
- No intrinsic absorption has been detected in any of the objects since the absorbing columns are always compatible with the Galactic values.
- Significant spectral curvature is present in the BeppoSAX spectra of most of the quasars and is related to the statistics of the observed spectrum: sources with the same energy index over the 0.1–10 keV band are fainter. The average curvature can be parameterized as a spectral flattening by $\Delta\alpha \sim 0.5 \pm 0.2$ towards high energies requiring two component models. The exact spectral shape and intensity of these components vary from object to object. In a few cases the curvature is due to a strong "soft excess" below about 1 keV, while for PG 1626+554, independent LECS–PSPC fits suggest the presence of an "ultra soft excess" (below 0.3 keV). The curvature in PG 1402+26 is mainly due to a hard tail above $\sim$ 5 keV rather than a "soft excess";
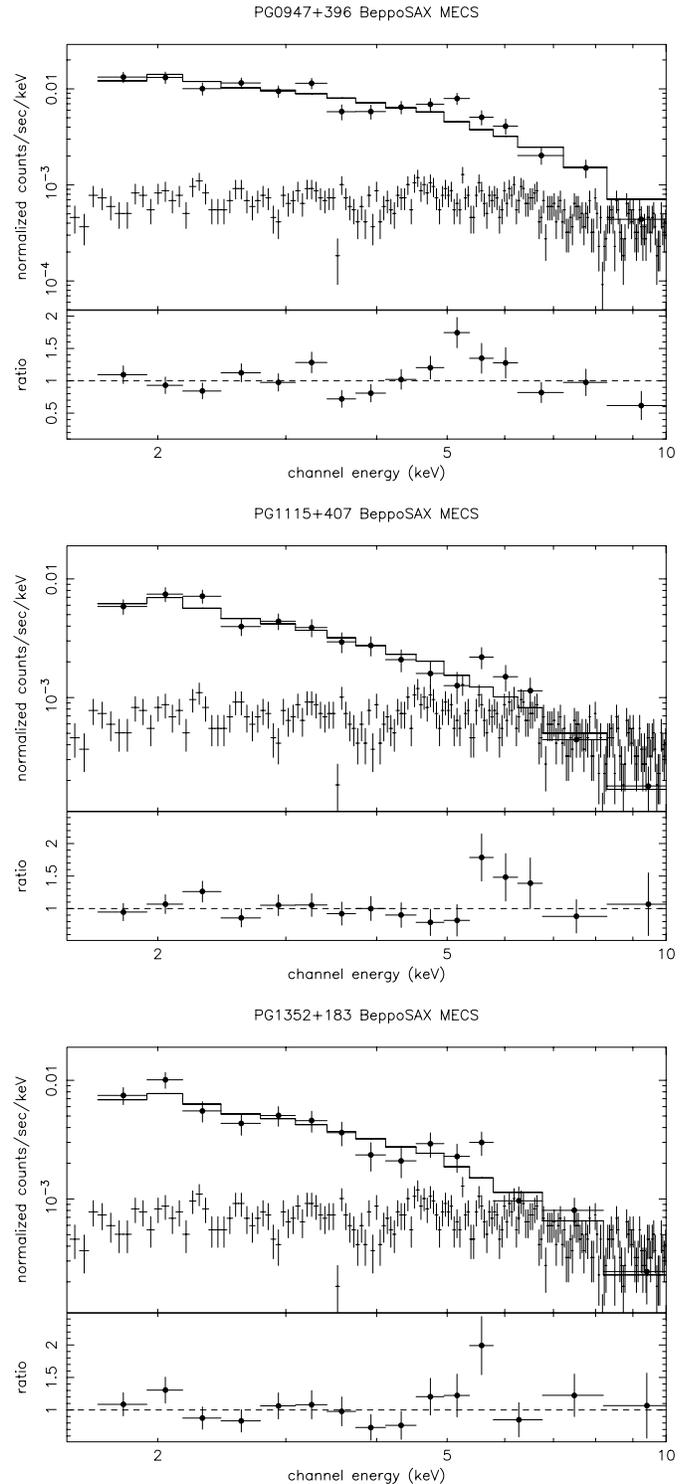
Fig. 5. PG 0947+396, PG 1115+407 and PG 1352+183 MECS spectra fitted with a single power law (superimposed as a continuous curve). For comparison the background is also shown. The lower panels represent data–to–model ratios.

also PG 1626+554 shows evidence for a hard tail. A spectral hardening at even higher energies ($>$ 10 keV) could be present in the two quasars detected in the PDS band.

- The origin of the spectral curvature is likely due to the combined effect of thermal emission from an accretion disk peaking in the far UV and the onset of a Compton reflection component at high energies. The addition of these components does provide a better description of the observed spectra. We also note that quasars with a steeper 0.1–2 keV spectrum tend to be steeper also in the 2–10 keV band, although the effect is detected only at the 68% confidence level.

- Iron K_α lines are detected in 4 quasars. The rest frame line energy (6.7 keV) and equivalent width (580 eV) of PG 1115+407 are consistent with those found in a few low redshift narrow–line Seyfert 1 galaxies (Comastri et al. 1998, Turner et al. 1998, Vaughan et al. 1999, Leighly 1999). The contemporaneous presence of a steep 0.1–10 keV continuum and narrow Hβ line allows us to classify this object as a relatively high redshift NLSy1.

  For the optically broad lined quasar PG 0947+396, the rest frame line energy of 6.4 keV is similar to that found in many local Seyfert 1 galaxies, suggesting fluorescence from cold iron. The line equivalent width (670 eV) is however higher (at the 2–3σ level) than that usually found in Seyfert 1 galaxies. We investigate the possibility that the high EW of the line, as well as an excess of counts detected in the PDS, are the result of fitting a complex continuum with a simple power-law model. We tried several other models (the inclusion of a Compton reflection component or of a thick and partial covering absorber) but in all cases the line is still required and its EW is never smaller than 400 eV.

  A line has also been detected in PG 1352+183 and PG 1226+023. In the first case the line energy and intensity are compatible with the values detected in many Seyfert galaxies. In the second case it could be witnessing a Seyfert-like spectrum diluted in the jet emission (Grandi et al. 1997, Haardt et al. 1998).

  The detection of significant Fe K–shell emission in 3 radio–quiet quasars with 2–10 keV luminosities in the range 1–5 × 10^{44} erg s^{-1} seems to be inconsistent with the trend seen in other radio–quiet AGN (Iwasawa & Taniguchi 1993; Nandra et al. 1997, George et al. 2000), where iron lines are more frequently found in lower luminosity objects.

- A detailed comparison with the recent ASCA observations of a larger sample of radio–quiet quasars (George et al. 2000) is not possible owing to the different responses, sensitivities and energy ranges covered by ASCA and BeppoSAX. We note however that there is a good agreement between the two samples especially for what concerns the average 2–10 keV slope and intrinsic dispersion and the presence of curved convex spectra in most of the objects. The detection with BeppoSAX of a strong iron line in a few relatively high luminosity objects deserves further investigation. The foreseen XMM-Newton quasar surveys will most likely settle several open issues.
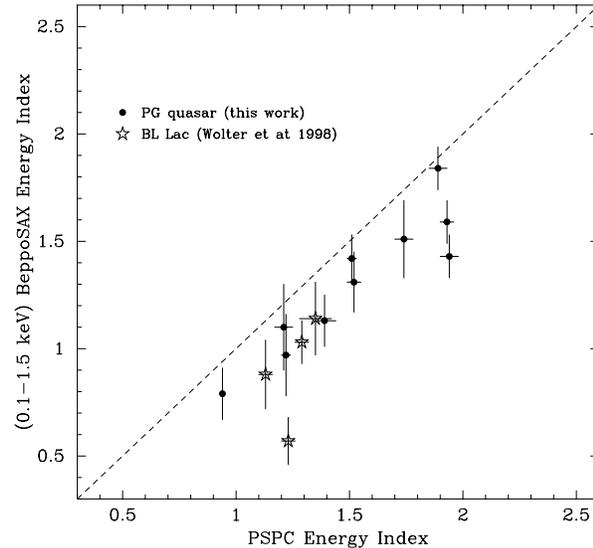
Fig. A.1. LECS energy index α_{LECS} detected in the energy range 0.1–1.5 keV vs the PSPC energy index α_S(PSPC) for the observed quasars plus four BL Lacs objects from the sample of Wolter et al. (1998)

Appendix A: comparison with PSPC

The discrepancy between the BeppoSAX soft spectral index and the PSPC one can be due to systematic errors in the instrument intercalibration. To investigate this discrepancy we fitted the LECS spectra in the energy range 0.1–1.5 keV with a power law plus Galactic absorption. Considering the different response curves of the two instruments around 1 keV (the LECS effective area increases from 1 to 2 keV, the PSPC area decreases in the same range) this is the LECS range which is more appropriate for a quantitative comparison with the PSPC. For the PG 1226+023 and PG 1202+281 fits we have added an edge at 0.6 keV and 0.8 keV respectively in the model. The resulting energy indices (α_{LECS}) are shown in Fig. A.1 as a function of the PSPC ones, together with the $\alpha_{LECS} = \alpha_S$(PSPC) line. To increase the sample we have added four BL Lacertae objects observed by BeppoSAX (Wolter et al. 1998). BL Lacs objects usually do not show large neutral or ionized low energy absorption (unlike Seyfert 1 and 2 galaxies) The four BL Lacs were selected from the ten of the Wolter et al. sample, excluding the objects with a complex (or variable) soft X-ray spectrum.

A systematic difference between the LECS and PSPC spectral indices is again evident. The BeppoSAX soft spectral indices vs the PSPC ones can be well fitted by a line with slope m=0.97±0.10 and offset $\Delta\alpha_E$=-0.23±0.16. Fixing m to 1 gives a constant difference between the two detectors measurements of $\Delta\alpha_E = -0.27 \pm 0.03$. Excluding the most discrepant point makes a marginal difference.

This discrepancy is smaller than that found between the PSPC and the Einstein IPC ($\Delta\alpha$=0.5; Fiore et al. 1994) and the
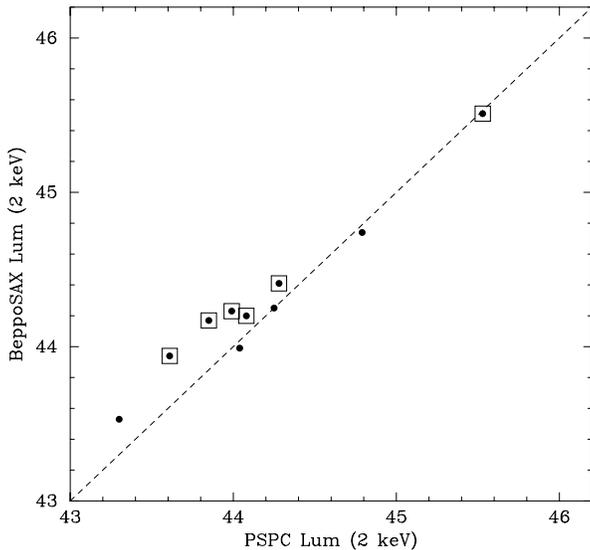
Fig. A.2. The 2 keV luminosity estimated from the BeppoSAX observations as a function of the PSPC 2 keV luminosity. Values are expressed in unit of log (erg s^{-1}).Points marked with squares represent the six quasars where a spectral curvature is present

one between the PSPC and the ASCA SIS ($\Delta\alpha = 0.4$; Iwasawa et al. 1999). In these latter two cases part of the difference can be due to the fact that the common energy range between these instruments is not large. Conversely, the energy range shared by the PSPC and the LECS is wide (0.1–2 keV), and, in particular, both instruments have good sensitivity below the Carbon edge at 0.28 keV. Their comparison is therefore more straightforward. However, if quasar spectra deviate from the simple power law, a small difference in the spectral index measured by the two instruments, that look at different average energies, could be possible. In order to check this effect we have fitted the LECS and PSPC spectra of the quasars with the best photon statistics simultaneously with curved models (broken power law and the power law with energy index variable with energy presented in Laor et al. 1994), allowing for a different normalization in the two instruments and letting the model parameters linked together.

The discrepancy in the estimated spectral index of about 0.2 could result from the differences in instrument response functions coupled with an energy dependent spectral slope at 0.1–2 keV (with a reasonable curvature) in about half of the cases. It is unclear then that the PSPC and BeppoSAX results are always inconsistent.

Fig. A.2 shows the BeppoSAX 2 keV luminosity as a function of the PSPC 2 keV luminosity. Six quasars have BeppoSAX luminosities slightly higher than PSPC luminosity: the BeppoSAX average luminosity is 30% higher than the PSPC one. Variability can certainly play a role in this difference, given the small sample of objects. However we note that 2 keV are the limit of the PSPC band and therefore a small uncertainty on the PSPC spectral shape could translate in a relatively large error on the 2 keV flux and luminosity. The slope of the correlation in Fig. A.2 is consistent with 1, indicating that this possible shift

should not alter the results of the correlations between luminosity and other quasar properties discussed in Laor et al. (1997).

References

Boella G., Butler R.C., Perola G.C., et al., 1997a, A&AS 122, 299
Boella G., Chiappetti L., Conti G., et al., 1997b, A&AS 122, 327
Boller T., Brandt W.N., Fink H.H., 1996, A&A 305, 53
Brandt W.N., Laor A., Wills B.J., 2000, astro-ph/9908016
Brandt W.N., Mathur S., Elvis M., 1997, MNRAS 285, L25
Chiappetti L., Cusumano G., Del Sordo S., et al., 1998, in: Scarsi L., Bradt H., Giommi P., Fiore F. (eds.), The Active X-ray Sky, Nuclear Physics B Proc. Suppl. 69/1-3, 610
Ciliegi P., Maccacaro T., 1997, MNRAS 292, 338
Ciliegi P., Maccacaro T., 1996, MNRAS 282, 477
Comastri A., Fiore F., Guainazzi M., et al., 1998, A&A 333, 31
Comastri A., Setti G., Zamorani G., et al., 1992, ApJ 384, 62
Ebeling H., Voges W., Bohoringer H., et al., 1996, MNRAS 281, 799
Elvis M., Fiore F., Siemiginowska A., Bechtold J., Mathur S. McDowell J.C.M., 2000, ApJ, submitted
Elvis M., 1992, in: Y. Tanaka Y., Koyama K. (eds.), Frontiers of X-ray Astronomy. Tokyo: Univ Acad. Press Inc., p. 567
Fiore F., La Franca F., Giommi P., et al., 1999a, MNRAS 306, L55
Fiore F., Guainazzi M., Grandi P., 1999b, ftp://www.sdc.asi.it/pub/sax/doc/software_docs/saxabc_v1.2.ps.gz
Fiore F., Mineo T., Laor A., Giallongo E., 1998, in: Scarsi L., Bradt H., Giommi P., Fiore F. (eds.), The Active X-ray Sky, Nuclear Physics B Proc. Suppl. 69/1-3, p. 529
Fiore F., Elvis M., McDowell C., Siemiginowska A., Wilkes B., 1994, ApJ 431, 515
Frontera F., Costa E., Dal Fiume D., et al., 1997, A&AS 122, 357
George I.M., Turner T.J., Yaqoob T., et al., 2000, ApJ (in press) astro-ph/9910218
Grandi P., Guainazzi M., Mineo T., et al., 1997, A&A 325, L17
Haardt F., Fossati G., Grandi P., et al., 1998, A&A 340, 35
Iwasawa K., Fabian A.C., Nandra K., 1999, MNRAS 307, 611
Iwasawa K., Taniguchi Y., 1993, ApJ 370, L61
Kellermann K.I., Saramek R., Schmidt M., Shaffer D.B., Green R., 1989, AJ 98, 1195
Laor A., Fiore F., Elvis M., et al., 1997, ApJ 477, 93
Laor A., Fiore F., Elvis M., et al., 1994, ApJ 435, 611
Lawson A.J., Turner M.J.L., 1997, MNRAS 288, 920
Leighly K.M., 1999, APJS 125, 317
Levine A.M., Lang F.L., Lewin W.H.G., et al., 1984, ApJS 54, 581
Maccacaro T., Gioia I.M., Wolter A., Zamorani G., Stocke J.T., 1988, ApJ 326, 680
Manzo G., Giarrusso S., Santangelo A., et al., 1997, A&AS 122, 341
Morrison R., McCammon D., 1983, ApJ 270, 119
Nandra K., George I.M., Mushotzky R.F., et al., 1997, ApJ 488, 91
Nicastro F., 2000, ApJ (in press) astro-ph/9912524
Orr A., Yaqoob T., Parmar A.N., et al., 1998, A&A 337, 685
Parmar A.N., Oosterbroek T., Orr A., et al., 1998, A&AS 136, 407
Parmar A.N., Martin D.D.E., Bavdaz M., et al., 1997, A&AS 122, 309
Pounds K.A., Done C., Osborne J.P., 1995, MNRAS 277, L5
Reeves J.N., Turner M.J.L., Ohashi T., Kii T., 1997, MNRAS 292, 468
Schmidt M., Green R.F., 1983, ApJ 413, 116
Stocke J.T., Morris S.L., Gioia I.M., et al., 1991, ApJS 76, 813
Stocke J.T., Liebert J., Schmidt G., et al., 1985, ApJ 289, 619
Turner T.J., George I.M., Nandra P., 1998, ApJ 508, 648
Ulrich-Demoulin M.H., Molendi S., 1996, ApJ 457, 77
Vaughan S., Reeves J., Warwick R., Edelson R., 1999, MNRAS 309, 113
Williams O.R., Turner M.J.L., Stewart G.C., et al. 1992, ApJ 389, 157
Wolter A., Comastri A., Ghisellini G., et al., 1998, A&A 335, 899
Yuan W., Brinkmann W., Siebert J., Voges W., 1998, A&A 330, 108